Article

Bioreduction of Gold Ions under Greener Conditions by the Thiol-Modified M13 Bacteriophage and with Hydroxylamine as the Autocatalytic Reducing Agent

Zongwu Wei,* Xueyan Wei, Chenxi Zhao, Han Zhang, and Zhenkun Zhang*

Read Online

ACCESS | Metrics & More | Article Recommendations | SI Supporting Information

ABSTRACT: Bioreduction of gold ions by the thiol-modified M13 bacteriophage (M13-SH) has been exploited as the potential alternative to conventional methods based on toxic chemicals, due to the gold affinity of the thiol groups, inherent gold reduction, and high specific surface area of the filamentous virus. Such efforts have been hindered by harsh conditions involving strong reducing agents and extreme pH that are harmful to the virus. Herein, a virus-friendly and greener method of bioreduction of $AuCl_4^-$ at neutral pH based on M13-SH is demonstrated. M13-SH was prepared by coupling the virus with N-succinimidyl S-acetylthioacetate, followed by deacylation in the presence of hydroxylamine·HCl to expose the thiol groups. The key finding is that without time-consuming purification, the mixture after deacylation consisting of M13-SH, residual hydroxylamine, and so forth can directly turn ionic gold species into gold, leading to macroscopic precipitated products with interconnected linear structures consisting of fused gold nanoparticles. Besides working as the virus-friendly reducing agent with a unique autocatalytic style, hydroxylamine diminishes disulfide bonding-induced intervirus bundling of M13-SH so as to maintain its efficient biosorption of ionic gold precursors. This work demonstrates a general and green strategy of bioreduction of gold via combination of the gold-affinity proteins or organisms and the unique autocatalytic reduction of hydroxylamine.
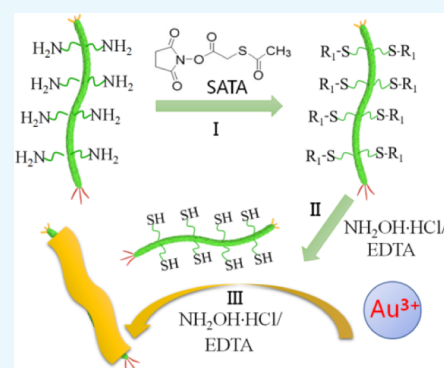
1. INTRODUCTION

Cyanide-based gold extraction from ores is a century-old technique. Due to stringent environmental regulations, it is compelling to develop alternative methods that can replace this efficient while extremely toxic method.[1] In addition, efficient recovery of the gold components from vast amounts of electronic wastes is another urgent challenge for a sustainable society.[2,3] One of the critical steps in gold extraction is reduction of gold ions to turn the soluble ionic gold species into pure gold, which often involve toxic chemicals and harsh conditions. Some greener strategies for such a step have been demonstrated, which still needed specific chemical agents and even had specific requirements for the salt form of the ionic gold precursors.[1,4−6] In contrast to these chemically based methods, bioreduction of gold ions by microorganisms such as bacteria, funguses, and viruses has been explored as the attractive alternative methods.[7−14] Especially, viruses such as the M13 bacteriophage and its mutants have garnered increasing attention in eco-friendly bioreduction of gold ions.[15−20]

With a diameter of ca. 6.6 nm and a length of ca. 900 nm, the M13 virus comprises a circular single-stranded DNA encapsulated in a filamentous proteinous capsid that consists of ca. 2700 major p8 coat proteins arranged in a helical way. Due to versatile possibilities of genetic engineering and chemical

modifications, M13 and its siblings have been intensively explored in advanced functional bionanomaterials.[15−22] Gold reduction using the M13 virus was first tried by Avery et al., while no gold was obtained at neutral pH.[23] Later on, Setyawati et al. reported that intact M13 alone can turn gold ions into gold nanoparticles while efficient gold retrial was only achieved at pH ∼ 3 and after long-term incubation.[24] Instead of acidic pH, Wang's group performed similar experiments at pH ∼ 12 and obtained discrete gold nanoparticles of a few nanometers in much shorter time.[25,26] These authors assumed that the ionic gold precursors absorbed onto the virus surface via nonspecific electrostatic interactions and were reduced into gold by the endogenous amino groups of the p8 coat protein.[24,25] If such a procedure was followed, gold products should have a linear structure consisting of aggregated gold particles along the rod-like virus.[17,18,20] However, the gold products in these works were often presented as plate-like or spherical nanoscale particles.[24,25] It was proposed that the virus
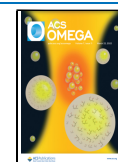
might attach to the surface of the particulate gold particles to stabilize them, whereas Wang's group observed that discrete gold nanoparticles stood side-by-side with intact filamentous viruses.[25] Therefore, efficient biosorption of the ionic gold precursors implemented by the high specific surface area inherent to the slender rod-like M13 has not manifested in these works. In addition, extreme pHs such as either pH ~ 3 or 12 were used to achieve effective gold recovery, which are harmful to the vulnerable M13 virus, especially during long-term incubation as often needed by virus-based gold reduction.[26,27]

Instead of the nonspecific electrostatic interactions of the ionic metal precursors with the virus surface, genetic manipulations of M13 have been explored to fuse the N-terminus of the p8 coat protein with the gold-affinity peptide fragments, which can promote highly efficient bioadsorption of gold ions onto the virus surface.[15−18] Laborious biopanning to screen gold-affinity mutants and constrained accessibility of the genetic techniques and so forth have limited the applications of such genetically engineered viruses. In contrast, chemical modification is a much versatile way to functionalize the M13 virus, thanks to the rich surface chemical groups of the solvent-exposed amino acid residuals of the p8 coat proteins.[20,28−31] Therefore, by exploring the well-known affinity of the thiol group for gold, M13 viruses modified with thiol groups (M13-SH) have been used as the efficient templates for gold reduction or assembling of preformed gold nanoparticles.[19,20,28,30,32] Convenience, versatility of chemical modifications and diverse metal affinity of the thiol groups are the advantages of M13-SH for gold extraction.[19,20,28,30,32]

In previous works based on either genetically engineered or thiol-modified viruses, the gold-affinity peptide tags or thiol groups promoted highly efficient biosorption of ionic gold precursors onto the virus surface, which were in most cases reduced into gold by such strong reducing agents as NaHB₄.[15−20,28,30,32] This was confirmed by the linear structure of the end gold products consisting of discrete gold nanoparticles assembling along the virus surface.[32] However, the strong reducing capability of NaHB₄ and dramatic pH change could be harmful to the structure integrity of the virus.[32] In addition, Montalvan-Sorrosa et al. reported that the free thiol groups of M13-SH would form disulfide bonds during storing or gold reduction, leading to cross-linked bundles of viruses.[32] Such a fact is consistent with previous results that gold particles often sit on the outermost surface of virus bundles.[15−20,28,30,32] Intervirus bundling dramatically lowers the amount of free thiol groups and the specific virus surface area available for interacting with the precursors of metal ions. These challenges must be addressed, before the thiol-modified M13 viruses (M13-SH) can be explored as the promising candidate for green bioreduction of gold with the potential of large-scale applications.

With the abovementioned challenges in mind, herein we shall report a virus-friendly, greener bioreduction of gold ions based on the thiol-modified M13 bacteriophage (M13-SH) (Scheme 1). Normally, the thiol groups are chemically coupled to the virus surface via reacting the amino groups on the virus surface with N-succinimidyl esters of the acetyl-protected sulfhydryl group such as N-succinimidyl S-acetylthioacetate (SATA).[20] To release the thiol group, a deacetylation process must be performed to remove the acetyl group, as often realized by hydroxylamine·HCl.[20] After time-consuming purification from the deacetylation mixture to remove residual

Scheme 1. Schematic Illustration of Bioreduction of Gold Ions Based on the Thiol-Modified M13 Bacteriophage; (I) Chemical Modification of the M13 Virus with SATA; (II) Deacetylation of the SATA-Modified Viruses by NH₂·HCl/EDTA; and (III) Bioreduction of Gold Ions by the Reaction Mixture after Deacetylation; R₁ Refers to the Acetyl Group
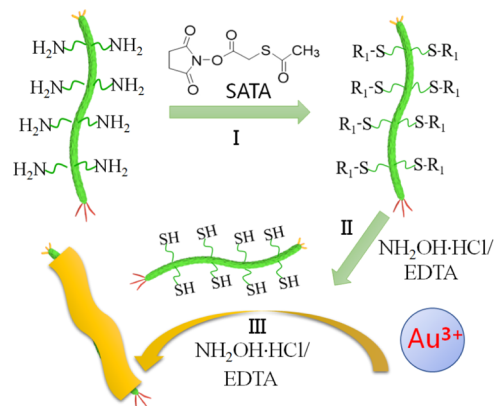
hydroxylamine and other chemicals, M13-SH was used for subsequent applications in binding with gold nanoparticles or as anchors for other chemical reactions.[16,17,23,25,26] Besides acting as the effective deacetylating agent, hydroxylamine has the unique property to reduce gold ions into gold but only works in the presence of preformed gold materials.[33,34] Furthermore, electroless deposition of gold onto protein assemblies with preloaded gold particles has confirmed that hydroxylamine is a biologically friendly reducing agent.[11,35,36] Based on these facts, we reckon that the mixture after deacetylation of the SATA-modified M13 viruses could be directly used for the gold extraction and there is no need to remove the residual hydroxylamine or other agents (Scheme 1). Hydroxylamine remained in the mixture after deacetylation is expected to prevent the nearly freed thiol groups on the virus surface from forming disulfide bonds that lead to cross-linked intervirus bundling so as to maintain the efficient biosorption of gold ions by M13-SH. Furthermore, hydroxylamine could play the role of reducing agents to replace NaHB₄.[37] As expected, our results demonstrated that the mixture after deacetylation consisting of M13-SH, hydroxylamine, and other chemicals could effectively transfer gold ions into gold at neutral pH. Gold products with interconnected linear structures consisting of fused gold particles were obtained, following a unique mechanism of biosorption of ionic gold species, initial self-reduction, and accelerated deposition by hydroxylamine reduction.

2. EXPERIMENTAL SECTION

2.1. Chemicals. SATA, hydroxylamine hydrochloride (NH₄OH·HCl), and ethylenediaminotetraacetic acid (EDTA) were provided by J&K chemical, Absin Bioscience Inc, and Heowns, respectively. Hydrogen tetrachloroaurate hydrate (HAuCl₄·3H₂O), sodium borohydride (NaHB₄), and other solvents were obtained from J&K chemical (Beijing, China) and used without further purification. The M13 virus was prepared following standard biochemical protocols. All of the chemical and agents for the preparation of the M13 virus were ordered from Dingguo Changsheng Bioscience Inc. (Beijing, China). Ultrapure water (18.2 mΩ·cm⁻¹) was always prepared using a Milli-Q Ultrapure system (Millipore).
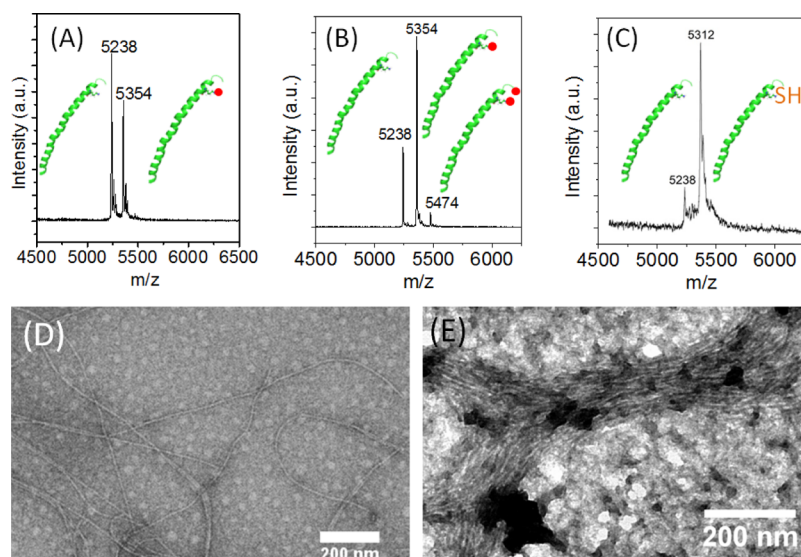
Figure 1. Characterizations of M13-SATA before and after deacetylation. MALDI-TOF MS of M13-SATA obtained at the SATA/p8 coat protein molar ratio of 5 (A) and 10 (B), respectively, as well as thiol-modified M13 resulted from deacetylation (C). The red dots in the insets represent the SATA moieties on each p8 coat protein. (D,E) TEM images of M13-SATA and M13-SH, respectively.

2.2. Modification of M13 with SATA. The procedure to couple SATA onto the M13 virus to prepare M13-SATA was based on previous work with some modifications.[20] The M13 virus was dispersed into phosphate buffer (100 mM, pH 7.4) to obtain a suspension containing 2 mg mL^{-1} M13. SATA was dissolved in anhydrous dimethyl sulfoxide (DMSO) to obtain the SATA solution. The concentration of SATA in DMSO was controlled to vary the molar ratio of the SATA to the p8 coat protein. Typically, 10 mL of the M13 suspension was incubated in a bath of water and ice at a temperature of ca. 4 °C, to which 250 μL of SATA solution in DMSO was added dropwise under vigorously stirring. After this step, the mixture was brought to room temperature and further incubated for 2 h with gentle magnetic stirring. The mixture was then dialyzed against phosphate buffer (100 mM, pH 7.4) in a dialysis tube with an MWCO of 12 KDa. The product of M13-SATA was further purified by ultracentrifugation and redispersion in the same phosphate buffer.

2.3. Deacetylation of M13-SATA to Prepare Thiol-Modified M13 Viruses. The acetyl groups of the SATA moieties coupled to the virus surface can be removed by hydroxylamine·HCl to expose the thiol group (Scheme S1 in the Supporting Information). The solutions for deacetylation consisted of 0.5 M hydroxylamine·HCl and 25 mM EDTA in phosphate buffer (100 mM, pH 7.4). The solution for deacetylation was mixed with M13-SATA in the same phosphate buffer in a volume ratio of 1: 10. The mixture was magnetically stirred at room temperature for 2 h. After this step, experiments of gold retraction can be directly tested with such a mixture. For other characterizations, the mixture after deacetylation was dialyzed against phosphate buffer (100 mM, pH 7.4) containing 10 mM EDTA to prevent oxidation-induced formation of disulphide bonding.

2.4. Gold Reduction Using the Mixture after Deacetylation of M13-SATA. All of the experiments were performed with M13-SATA obtained at the molar ratio of SATA to the p8 coat protein of 10:1. The mixture after the deacetylation reaction performed for 2 h as presented in 2.2 was used to test the gold reduction. At this stage, the mixture

mainly consisted of 0.2 mg mL^{-1} M13-SH and residual hydroxylamine, with a pH of ca. 7.4. HAuCl$_4$ was added to the mixture after deacetylation to approach a concentration of 670 μM. The mixture was shaken in the dark in a temperature-controlled incubator at 37 °C and at a shaking speed of 200 rpm. To quench the reaction, the mixture was dialyzed against a large amount of phosphate buffer at pH of 7.4 and then ultrapure water. The dialyzed mixture was centrifuged at 25,000g to collect the viruses or potential gold products. Samples for the TEM characterizations were prepared from the product from centrifugation.

2.5. Monitoring of the Procedure of Gold Reduction by the Mixture after Deacetylation of M13-SATA. Following the procedure presented in 2.3, the mixture for gold reduction was prepared and shaken at 37 °C with a shaking speed of 200 rpm. Aliquots of samples were taken at an interval of each hour and directly used for recording of the adsorption spectra by UV–vis measurements. Small part was dialyzed against a large amount of PB buffer and ultrapure water to quench any reactions and remove any chemicals. The as-processed mixture was centrifuged at 25,000g to collect the viruses or potential gold particles and the precipitates were then redispersed in ultrapure water. Samples for the TEM characterizations were prepared from the product from centrifugation.

2.6. Characterizations. MALDI-TOF mass spectrometry of the wild, SATA-modified M13 viruses before and after deacetylation was measured on the AutoflexIII LRF200-CID matrix-assisted laser desorption/ionization-time-of-flight (MALDI-TOF) mass spectrometry (MS) (Bruker Daltonics, Germany). The Kratos AXIS-ULTRA DLD high-performance XPS system (Kratos Analytical Ltd) was used for XPS analysis. TEM, high-angle annular dark field (HAADF), and energy-dispersive spectroscopy (EDS) measurements were performed on an FEI Talos F200X G2 TEM (Thermo Scientific). Samples for TEM were normally stained with 2% uranyl acetate unless otherwise noted. Dynamic light scattering was carried out on a BeNano 90 Zeta (Bettersize Instruments Ltd., Dandong, China). All of the absorbance spectra were recorded

on a Shimadzu UV–vis 2550 spectrometer. Centrifugation and ultracentrifugation were performed either on an Allegra X-15R with an FX6100 fixed angle rotor or an Optima L-90K with a Ti-90 rotor (Beckman Coulter), respectively.

3. RESULTS AND DISCUSSION

The thiol groups were chemically coupled to the virus surface via reacting SATA with the solvent-accessible amino groups of the p8 coat protein (Scheme S1 in the Supporting Information). The SATA-modified virus (M13-SATA) was first characterized by MALDI-TOF MS (Figure 1A).[30] Besides the m/z peak of the native p8 coat protein at 5238, a new peak appeared at 5354, corresponding to one p8 coat protein coupled with one SATA moiety.[19] The amount of SATA moieties per virus can be controlled by increasing the molar ratio of SATA to the p8 coat protein (SATA/p8). For instance, at the SATA/p8 of 10:1, there appeared new peaks assigned to one p8 coat protein coupled with one or two SATA moieties, while the intensity of the peak assigned to the native p8 decreased (Figure 1B). To expose the free thiol groups, M13-SATA was subjected to deacetylation in neutral phosphate buffer containing $NH_2OH \cdot HCl$ and EDTA.[20] Successful deacetylation of the SATA moieties on the virus was also conveniently confirmed by MALDI-TOF MS, as indicated by the new m/z peaks at 5312 and 5386, which are assigned to one p8 coat protein bearing one or two thiol groups (Figure 1C). These results are consistent with previous works.[19] TEM revealed the filamentous morphology of M13-SATA with a length of 900 nm and a diameter of 6.6 nm, confirming the structure integrity of the virus after the SATA modification (Figure 1D). For the M13 virus bearing free thiol groups (M13-SH) after purifying from the deacetylation mixture and storing in pure PBS buffer for some times, one interesting discovery is that M13-SH formed bundles consisting of multiple viruses (Figures 1E and S1 in the Supporting Information). Apparent hydrodynamic diameters obtained from dynamic light scattering also indicated larger aggregates formed in the suspension of M13-SH (Figure S1C in the Supporting Information). As reported by others, the thiol groups on the virus surface can form disulfide bonds via oxygen-catalyzed oxidation and intervirus disulfide bonding leads to cross-linked bundles of several viruses.[32] Such bundling will dramatically decrease the amount of free thiol groups and the specific viral surface available for biosorption of gold ions, which are the reason of the lower-than-expected gold bioreduction efficiency. Such a fact is consistent with previous results that gold particles often sit on the outermost surface of virus bundles.[15−20,28,30,32] We believed that one of the effects of the strong reducing agent $NaHB_4$ used in most of the previous works was to cleave such disulfide bonds into free thiol groups.[32]

To demonstrate our idea that the reacting mixture after deacetylation of M13-SATA can be directly used for gold reduction without any further purification, the gold source tetrachloroauric acid ($HAuCl_4$) was added to the reaction mixture after deacetylation that contained the M13 virus bearing free thiol groups (M13-SH), residual NH_3OH, and some EDTA in PBS buffer of pH ∼ 7.4. The M13-SATA used was the one obtained at the SATA/p8 molar ratio of 10 to 1 (M13-SH10) which have large amounts of free thiol groups on the virus surface (Figure 1B). During incubation, the color of the reaction mixture turned from a pale yellowish to purple, while visible precipitates gradually appeared (Figure 2D). TEM
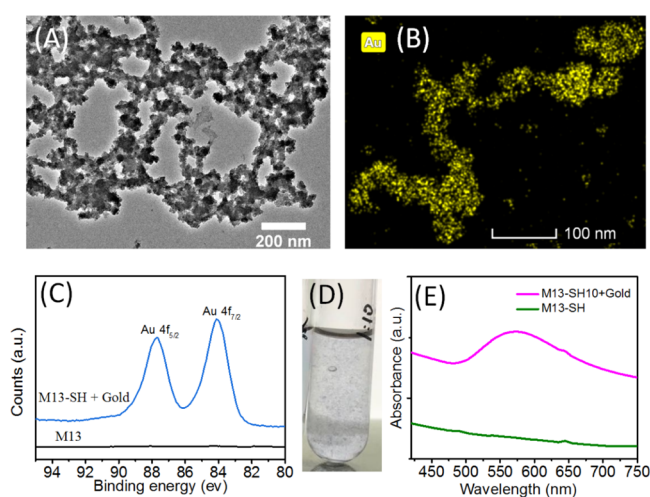

Figure 2. Characterizations of the gold products obtained from reduction of gold ions by the reaction mixture after deacetylation of M13-SATA. (A) TEM characterizations; (B) elemental mapping of the gold products by EDS; and (C) high-resolution scanning of Au 4f in the scanning survey of XPS. (D) Appearance and (E) optical absorption spectra of the suspension after gold bioreduction and the thiol-modified M13 (M13-SH).

revealed that the precipitates are interconnected linear aggregates, consisting of fused gold nanoparticles with an irregular shape (Figure 2A). Elemental mapping by EDS confirmed that these aggregates contain gold element (Figures 2B and S2 in the Supporting Information), the oxidation state of which was further determined by X-ray photoelectron spectroscopy (XPS) (Figures 2C and S3 in the Supporting Information). Doublet signal peaks of $4f_{7/2}$ at 84.07 eV and $4f_{5/2}$ at 87.77 eV corresponding to Au^0 existed in the high-resolution scanning of Au 4f of the XPS scanning survey (Figure 2C).[38] In addition, the final mixtures have a broad absorption in the range of 500 to 700 nm, with an asymmetric peak centering at ca. 560 nm and a long wavelength tail extending beyond 900 nm (Figure 2E). As suggested by previous works, such optical absorption stemmed from the surface plasma resonance (SPR) of gold nanoparticles with anisotropic structures such as gold nanoparticles assembled in a linear form.[18,20,39]

To corroborate with the abovementioned discovery, control experiments were performed under similar conditions (as detailed in the Supporting Information). At first, the M13 bearing free thiol groups (M13-SH) was purified from hydroxylamine and other chemical agents and then incubated with $HAuCl_4$ at neutral pH in the absence of any reducing agents. Similarly, M13-SATA without experiencing deacetylation was subjected to the same conditions of gold extraction. In addition, the intact M13 virus was dispersed in the deacetylation mixture and tested for gold extraction either in the absence or presence of hydroxylamine. For all these cases, there was no visible precipitate and only some gold nanoparticles with an irregular shape were observed after long-term incubation (>72 h) (Figure 3). Finally, gold reduction was tested with the remaining mixture that only consisted of residual hydroxylamine, EDTA, and so forth after deacetylation and removing the thiol-modified M13. No gold species can be observed after long-term incubation. Results from these experiments suggest that both the thiol-modified
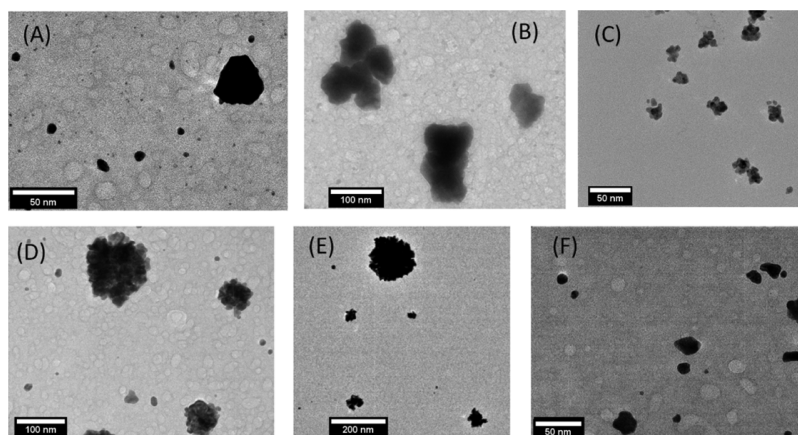
Figure 3. Control experiments of gold reduction. (A) M13-SATA dispersed in pure phosphate buffer in the absence of $NH_2OH \cdot HCl$/EDTA. (B) Thiol-modified M13 (M13-SH) from deacetylation of M13-SATA dispersed in pure phosphate buffer in the absence of $NH_2OH \cdot HCl$/EDTA. (C,D) Wild-type M13 virus dispersed in pure phosphate buffer and in the absence (C) and presence (D) of $NH_2OH \cdot HCl$/EDTA. (E) Wild-type M13 virus dispersed the supernatant from the deacetylation mixture after removing the thiol-modified M13. (F) Supernatant from the deacetylation mixture after removing the thiol-modified M13.

M13 virus and hydroxylamine play critical roles in effective bioreduction of gold ions at neutral pH.

To have certain insights into the mechanism of gold reduction at neutral pH by the reaction mixture after deacetylation of M13-SATA, we monitored the reduction procedure right after adding $HAuCl_4$ into the mixture of deacetylation by both UV−vis spectroscopy and TEM (Figure 4). Some unique characteristics were revealed by the
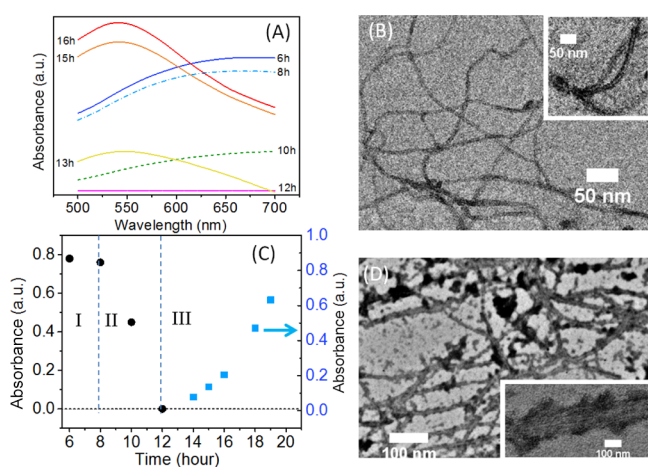

Figure 4. UV−vis spectroscopy (A) and TEM characterization during gold reduction by the reaction mixture of deacetylation of M13-SATA. (A) Absorption spectra at several typical times. The spectra less than 12 h were recorded directly in the reaction mixture while these after 12 h were recorded from the collected precipitates after redispersing in buffer. (C) Relative intensity at the absorption peaks of (A) vs the reduction times. (B,D) TEM images of the viruses collected at 8 and 12 h, respectively.

absorption behaviors in the range of 500−700 nm recorded at several typical times (T_r) (Figure 4A). Especially, the time-dependent relative intensity at each absorption peak can be roughly divided into three stages (Figure 4C). At $T_r < 12$ h, the broad absorption mainly occurred in the wavelength range of 600 to 700 nm, which should be contributed by thiol-modified M13 viruses (M13-SH), $AuCl_4^-$, NH_4OH, and so forth, or light scattering by the rod-like viruses. Starting from $T_r \sim$ ca.

10 h, the absorption intensity in the long-wavelength range sharply decreased and visible precipitates appeared. After the precipitates settled to the bottom of the containers at $T_r \sim 12$ h, no pronounced absorption can be detected from the supernatant. The precipitates should be the gold products containing viruses, leading to decreased contents of the virus, $AuCl_4^-$, NH_4OH, and so forth in the supernatant and therefore diminished absorption. Interestingly, after redispersing the precipitates collected since $T_r > 12$ h in PB buffer, there were clear absorptions in the lower-wavelength range of 500−600 nm with peaks around 530−560 nm. The relative intensity at the absorption peaks increased upon increasing times, which should stem from increasing amounts of gold products (the third stage in Figure 4C). TEM characterization without heavy metal staining of the samples taken during the first stage indicated enhanced contrast of the virus, suggesting effective adsorption of the gold ions along the virus surface (Figure 4B). For the one sampled at the second stage, there is a clear layer of gold that is unevenly distributed along the virus surface (Figure 4D).

It is well-recognized that NH_2OH can thermodynamically reduce Au^{3+} into gold.[34] However, such a capability only works efficiently in the presence of preformed gold surfaces that can accelerate the gold ion reduction by NH_2OH.[33,37] Therefore, this chemical has been employed as the reducing agent for deposition of gold onto the preformed Au nanoparticles or films.[33,37] Based on these facts, we tentatively propose the following mechanism (Scheme 1). The SATA moieties on the M13-SATA surface were turned into free thiol groups during deacetylation while the formation of disulfide bonds can be effectively avoided by residual hydroxylamine remained in the deacetylation mixture. The free thiol groups and the high specific surface area of the slender filamentous virus promote highly efficient biosorption of gold ions onto the surface of the virus (the first stage of Figure 4C). In the second stage of Figure 4C, the endogenous amino groups on the virus surface such as tyrosine, tryptophan, aspartic acid, glutamic acid, and so forth could reduce the absorbed god ions to form the first parts of gold.[24] However, as suggested by previous works, such a self-reduction procedure is extremely inefficient, especially at neutral pH.[24,25] In the current work, as soon as there was some gold formed along the virus surface, reduction of gold ions

would be dramatically accelerated by hydroxylamine even at neutral pH.[36] This could explain the prompt change in the absorbance behaviors occurred in the third stage of Figure 4C. The rugged and uneven distribution of the gold layer at this stage is also in line with the fact that gold deposition catalyzed by hydroxylamine preferably occurred to the regions where some preformed gold existed (Figure 4D).

In previous works, the thiol-modified M13 virus was first purified from the deacetylation mixture and then used for bioreduction of gold ions in the presence of the strong reducing agents such as NaHB$_4$ and the gold products mainly consist of discrete gold nanoparticles attached to the bundles of cross-linked viruses.[15−20,28,30,32] In contrast, the results of the current work clearly demonstrated that the reaction mixture after deacetylation of M13-SATA are efficient in bioreduction of gold ions at neutral pH and no need of strong reduction agents such as NaHB$_4$ and time-consuming purification. Especially, the precipitated gold products with interconnected linear-like structures of fused gold nanoparticles is distinct from that obtained using the thiol-modified M13 virus together with NaHB$_4$. In addition, such morphology of gold is also different from the plate-like or spherical gold nanoparticles obtained with the wild-type M13 virus under either strong acidic or alkaline conditions.[24,25] Finally, influence of NaBH$_4$ and hydroxylamine on the structural stability of the M13 phage was investigated (see the Supporting Information). Long-term incubation with NaBH$_4$ resulted in abnormal UV absorption phenomena and fragmentation of the M13 virus, while the structure of the virus was not influenced by hydroxylamine (Figure S4 in the Supporting Information). The strong reducing conditions using NaBH$_4$ often disrupt the structure of the virus by cleaving nascent disulfide bonds or denaturing the coat proteins.[32] These results indicated that hydroxylamine is a virus-friendly reducing agent.

4. CONCLUSIONS

In summary, without any time-consuming purification procedure, the mixture after deacetylation to free the thiol groups of the SATA-modified M13 virus can be directly used for reduction of gold ions. By incubating AuCl$_4^-$ at neutral pH with the mixture after deacetylation of the SATA-modified M13 virus, we obtained macroscopic precipitated gold products with interconnected linear structures consisting of fused gold nanoparticles. Investigations of the underlining mechanism reveals that the main components in the solutions after deacetylation, that is, the thiol-modified M13 virus and residual hydroxylamine, work synergistically to effectively turn gold ions into gold at neutral pH. The abundant thiol groups implement efficient bioadsorption of the gold ions onto the filamentous viruses which start the initial gold bioreduction with its endogenous amino acids. The residual hydroxylamine plays two critical roles by keeping the thiol groups from forming disulfide bonds while enhancing reduction of the gold ions through a unique autocatalytic way. By performing gold bioreduction under neutral and virus-friendly conditions, the current work excludes the harsh conditions involving strong reducing agents such as NaBH$_4$.

ASSOCIATED CONTENT

Supporting Information

The Supporting Information is available free of charge at https://pubs.acs.org/doi/10.1021/acsomega.2c00563.

Supplementary results and details for control experiments of gold reduction under other conditions, influence of NaHB$_4$ on the structural stability of the M13 virus, and investigation of intervirus bundling of thiol-modified M13 (PDF)

AUTHOR INFORMATION

Corresponding Authors

Zongwu Wei − *College of Resources, Environment and Materials, Guangxi University, Nanning, Guangxi 530004, China*; Email: weizongwu@gxu.edu.cn

Zhenkun Zhang − *Key Laboratory of Functional Polymer Materials of Ministry of Education, Institute of Polymer Chemistry, College of Chemistry, Nankai University, Tianjin 300071, China*; orcid.org/0000-0002-3480-2381; Email: zkzhang@nankai.edu.cn

Authors

Xueyan Wei − *College of Resources, Environment and Materials, Guangxi University, Nanning, Guangxi 530004, China*

Chenxi Zhao − *Key Laboratory of Functional Polymer Materials of Ministry of Education, Institute of Polymer Chemistry, College of Chemistry, Nankai University, Tianjin 300071, China*

Han Zhang − *College of Resources, Environment and Materials, Guangxi University, Nanning, Guangxi 530004, China*

Complete contact information is available at:
https://pubs.acs.org/10.1021/acsomega.2c00563

Notes

The authors declare no competing financial interest.

REFERENCES

(1) Zhang, Y.; Cui, M.; Wang, J.; Liu, X.; Lyu, X. A review of gold extraction using alternatives to cyanide: Focus on current status and future prospects of the novel eco-friendly synthetic gold lixiviants. *Miner. Eng.* **2022**, *176*, 107336.

(2) Syed, S. Recovery of gold from secondary sources—A review. *Hydrometallurgy* **2012**, *115−116*, 30−51.

(3) Bigum, M.; Brogaard, L.; Christensen, T. H. Metal recovery from high-grade WEEE: a life cycle assessment. *J. Hazard. Mater.* **2012**, *207−208*, 8−14.

(4) Yue, C.; Sun, H.; Liu, W.-J.; Guan, B.; Deng, X.; Zhang, X.; Yang, P. Environmentally benign, rapid, and selective extraction of gold from ores and waste electronic materials. *Angew. Chem.* **2017**, *129*, 9459−9463.

(5) Liu, Z.; Frasconi, M.; Lei, J.; Brown, Z. J.; Zhu, Z.; Cao, D.; Iehl, J.; Liu, G.; Fahrenbach, A. C.; Botros, Y. Y. Selective isolation of gold facilitated by second-sphere coordination with α-cyclodextrin. *Nat. Commun.* **2013**, *4*, 1855.

(6) Sun, D. T.; Gasilova, N.; Yang, S.; Oveisi, E.; Queen, W. L. Rapid, selective extraction of trace amounts of gold from complex water mixtures with a metal−organic framework (MOF)/polymer composite. *J. Am. Chem. Soc.* **2018**, *140*, 16697−16703.

(7) Lin, L.; Wu, W.; Huang, J.; Sun, D.; Waithera, N. u. M.; Zhou, Y.; Wang, H.; Li, Q. Catalytic gold nanoparticles immobilized on

yeast: from biosorption to bioreduction. *Chem. Eng. J. (Lausanne)* **2013**, *225*, 857−864.

(8) Shin, D.; Jeong, J.; Lee, S.; Pandey, B. D.; Lee, J.-c. Evaluation of bioleaching factors on gold recovery from ore by cyanide-producing bacteria. *Miner. Eng.* **2013**, *48*, 20−24.

(9) Tsuruta, T. Biosorption and recycling of gold using various microorganisms. *J. Gen. Appl. Microbiol.* **2004**, *50*, 221−228.

(10) Liu, Y.; Pei, R.; Huang, Z.; Xiao, J.; Yao, A.; Xu, K.; Li, Y.; Ullah, S.; Yu, Z.; Wang, Y.; Zhou, S.-F.; Zhan, G. Green immobilization of CdS-Pt nanoparticles on recombinant Escherichia coli boosted by overexpressing cysteine desulfurase for photocatalysis application. *Bioresour. Technol. Rep.* **2021**, *16*, 100823.

(11) Aljabali, A. A. A.; Lomonossoff, G. P.; Evans, D. J. CPMV-polyelectrolyte-templated gold nanoparticles. *Biomacromolecules* **2011**, *12*, 2723−2728.

(12) Shedbalkar, U.; Singh, R.; Wadhwani, S.; Gaidhani, S.; Chopade, B. A. Microbial synthesis of gold nanoparticles: current status and future prospects. *Adv. Colloid Interface Sci.* **2014**, *209*, 40−48.

(13) Mukherjee, P.; Ahmad, A.; Mandal, D.; Senapati, S.; Sainkar, S. R.; Khan, M. I.; Ramani, R.; Parischa, R.; Ajayakumar, P. V.; Alam, M.; Sastry, M.; Kumar, R. Bioreduction of AuCl4− ions by the fungus, Verticillium sp. and surface trapping of the gold nanoparticles formed. *Angew. Chem., Int. Ed.* **2001**, *40*, 3585−3588.

(14) Mata, Y.; Torres, E.; Blazquez, M.; Ballester, A.; González, F.; Munoz, J. Gold (III) biosorption and bioreduction with the brown alga Fucus vesiculosus. *J. Hazard. Mater.* **2009**, *166*, 612−618.

(15) Huang, Y.; Chiang, C.-Y.; Lee, S. K.; Gao, Y.; Hu, E. L.; Yoreo, J. D.; Belcher, A. M. Programmable assembly of nanoarchitectures using genetically engineered viruses. *Nano Lett.* **2005**, *5*, 1429−1434.

(16) Nam, K. T.; Kim, D.-W.; Yoo, P. J.; Chiang, C.-Y.; Meethong, N.; Hammond, P. T.; Chiang, Y.-M.; Belcher, A. M. Virus-enabled synthesis and assembly of nanowires for lithium ion battery electrodes. *Science* **2006**, *312*, 885−888.

(17) Manivannan, S.; Park, S.; Jeong, J.; Kim, K. Aggregation-free optical and colorimetric detection of Hg (II) with M13 bacteriophage-templated Au nanowires. *Biosens. Bioelectron.* **2020**, *161*, 112237.

(18) Ngo-Duc, T.-T.; Plank, J. M.; Chen, G.; Harrison, R. E. S.; Morikis, D.; Liu, H.; Haberer, E. D. M13 bacteriophage spheroids as scaffolds for directed synthesis of spiky gold nanostructures. *Nanoscale* **2018**, *10*, 13055−13063.

(19) Vera-Robles, L. I.; Escobar-Alarcón, L.; Picquart, M.; Hernández-Pozos, J. L.; Haro-Poniatowski, E. A biological approach for the synthesis of bismuth nanoparticles: using thiolated M13 phage as scaffold. *Langmuir* **2016**, *32*, 3199−3206.

(20) Vera-Robles, L. I.; Van Tran Nhieu, G.; Laberty-Robert, C.; Livage, J.; Sanchez, C. Flexible electroactive nanomaterials biotemplated with versatile M13 phage platforms. *Adv. Eng. Mater.* **2013**, *15*, 954−961.

(21) Han, L.; Shao, C.; Liang, B.; Liu, A. Genetically engineered phage-templated MnO2 nanowires: synthesis and their application in electrochemical glucose biosensor operated at neutral pH condition. *ACS Appl. Mater. Interfaces* **2016**, *8*, 13768−13776.

(22) Zhang, Z.; Buitenhuis, J. Synthesis of uniform silica rods, curved silica wires, and silica bundles using filamentous fd virus as a template. *Small* **2007**, *3*, 424−428.

(23) Avery, K. N.; Schaak, J. E.; Schaak, R. E. M13 bacteriophage as a biological scaffold for magnetically-recoverable metal nanowire catalysts: combining specific and nonspecific interactions to design multifunctional nanocomposites. *Chem. Mater.* **2009**, *21*, 2176−2178.

(24) Setyawati, M. I.; Xie, J.; Leong, D. T. Phage based green chemistry for gold ion reduction and gold retrieval. *ACS Appl. Mater. Interfaces* **2014**, *6*, 910−917.

(25) Wang, X.; Yang, T.; Zhang, X.; Chen, M.; Wang, J. In situ growth of gold nanoparticles on Hg 2+-binding M13 phages for mercury sensing. *Nanoscale* **2017**, *9*, 16728−16734.

(26) Wang, X.-Y.; Yang, J.-Y.; Wang, Y.-T.; Zhang, H.-C.; Chen, M.-L.; Yang, T.; Wang, J.-H. M13 phage-based nanoprobe for sers detection and inactivation of staphylococcus aureus. *Talanta* **2021**, *221*, 121668.

(27) Branston, S. D.; Stanley, E. C.; Ward, J. M.; Keshavarz-Moore, E. Determination of the survival of bacteriophage M13 from chemical and physical challenges to assist in its sustainable bioprocessing. *Biotechnol. Bioprocess Eng.* **2013**, *18*, 560−566.

(28) Peng, H.; Borg, R. E.; Dow, L. P.; Pruitt, B. L.; Chen, I. A. Controlled phage therapy by photothermal ablation of specific bacterial species using gold nanorods targeted by chimeric phages. *Proc. Natl. Acad. Sci. U. S. A.* **2020**, *117*, 1951−1961.

(29) Chung, W.-J.; Lee, D.-Y.; Yoo, S. Y. Chemical modulation of M13 bacteriophage and its functional opportunities for nanomedicine. *Int. J. Nanomed.* **2014**, *9*, 5825.

(30) Lee, J. H.; Domaille, D. W.; Cha, J. N. Amplified protein detection and identification through DNA-conjugated M13 bacteriophage. *ACS Nano* **2012**, *6*, 5621−5626.

(31) Cao, J.; Liu, S.; Xiong, J.; Chen, Y.; Zhang, Z. Stimuli responsive chiral liquid crystal phases of phenylboronic acid functionalized rodlike viruses and their interaction with biologically important diols. *Chem. Commun.* **2014**, *50*, 10402−10405.

(32) Montalvan-Sorrosa, D.; González-Solis, J. L.; Mas-Oliva, J.; Castillo, R. Filamentous virus decoration with gold nanoparticles: global fingerprints of bionanocomposites acquired with SERS. *RSC Adv.* **2014**, *4*, 57329−57336.

(33) Brown, K. R.; Natan, M. J. Hydroxylamine seeding of colloidal Au nanoparticles in solution and on surfaces. *Langmuir* **1998**, *14*, 726−728.

(34) Stremsdoerfer, G.; Perrot, H.; Martin, J. R.; Cléchet, P. Autocatalytic Deposition of Gold and Palladium onto n-GaAs in Acidic Media. *J. Electrochem. Soc.* **1988**, *135*, 2881.

(35) Radloff, C.; Vaia, R. A.; Brunton, J.; Bouwer, G. T.; Ward, V. K. Metal nanoshell assembly on a virus bioscaffold. *Nano Lett.* **2005**, *5*, 1187−1191.

(36) Wnęk, M.; Górzny, M. Ł.; Ward, M.; Wälti, C.; Davies, A.; Brydson, R.; Evans, S.; Stockley, P. Fabrication and characterization of gold nano-wires templated on virus-like arrays of tobacco mosaic virus coat proteins. *Nanotechnology* **2013**, *24*, 025605.

(37) Meltzer, S.; Resch, R.; Koel, B. E.; Thompson, M. E.; Madhukar, A.; Requicha, A. A. G.; Will, P. Fabrication of nanostructures by hydroxylamine seeding of gold nanoparticle templates. *Langmuir* **2001**, *17*, 1713−1718.

(38) Vasimalai, N.; John, S. A. Micromolar Hg (II) induced the morphology of gold nanoparticles: a novel luminescent sensor for femtomolar Hg (II) using triazole capped gold nanoparticles as a fluorophore. *J. Mater. Chem. A* **2013**, *1*, 4475−4482.

(39) Peng, H.; Chen, I. A. Rapid colorimetric detection of bacterial species through the capture of gold nanoparticles by chimeric phages. *ACS Nano* **2018**, *13*, 1244−1252.